Burrowing of Co nanoparticles on clean Cu and Ag surfaces

C. G. Zimmermann[1,2], M. Yeadon, K. Nordlund, J. M. Gibson and R. S. Averback
[1] *Materials Research Laboratory, University of Illinois, Urbana, IL 61801*

U. Herr and K. Samwer
[2] *Institut für Physik, Universität Augsburg, D-86135 Augsburg*

Metal nanoparticles can display a unique behavior when deposited on substrates with a significantly lower surface energy. Co nanoparticles in the 10 nm size regime burrow into clean Cu(100) and Ag(100) substrates when deposited at 600 K and also assume the substrate orientation. Deposition at room temperature fails to show either burrowing or reorientation. Crucial in understanding these results are the capillary forces and surface tension associated with a nanoparticle: they must be high enough to drive atoms away from underneath the cluster.

An abundance of evidence now demonstrates that the growth of epitaxial thin films does not necessarily follow one of the three classical modes (layer-by-layer, agglomeration, two-dimensional growth followed by island growth). A specific example is the case of a metal grown on a single crystalline substrate of much lower surface energy than itself. One monolayer of Ni deposited on Ag(111) or Ag(100), in particular, becomes covered by one or two layers of Ag upon annealing to 770 K and 620 K respectively. [1,2] . Theoretical calculations [2–4], predict, moreover, that these capping layers remain on top during further deposition. Monte-Carlo simulations [5] show that a Ni monolayer upon annealing to 620 K spreads over 6 – 7 subsurface layers in the form of clusters with (111) and (100) facets which contain about 100 atoms. Similar behavior was observed when 20 monolayers of Co were epitaxially grown on Cu(100) at room temperature [6]. Upon annealing to 670 K a capping layer of Cu formed by diffusion of substrate Cu atoms through "pinholes", step bands and the like, onto free surfaces of the Co film [6,7]. In the early stages of this growth, STM studies revealed that Co forms triangular double-layer islands on Cu(111) with a Cu overlayer at 300 K [8,9]. These islands also occupy one subsurface layer. Lastly, we note that when pure Co is deposited on Cu between 700 and 900 K, a Co-Cu alloy grows on the surface, even though these metals are nearly immiscible in equilibrium [10]. There Cu flows from the bottom of the film through pinholes and mixes with the arriving Co.

This letter reports on observations of a related, but new phenomenon, concerning the deposition of nanoparticles on single crystalline films. We find that Co nanoparticles with diameters of $\approx$ 10 nm do not remain on the surface of Cu(100) and Ag(100) films when deposited at 600 K, but rather they burrow into these substrates. This behavior is fundamentally different from the capping behavior in the work cited above, since it is driven, as we will show, by the exceptionally large capillary forces rather than the differences in surface free energies. The fact that Co has a larger surface energy than either Cu or Ag, predicts only the formation of a thin layer of substrate material around the particles, but not burrowing. We further observe that the Co nanoparticles reorient to become coherent with the Cu matrix as they sink, whereas they only become semi-coherent in the case of Ag. These findings imply that burrowing is rather general and that it is in fact a mechanism of surface smoothing that has not been previously considered. Burrowing also has obvious implications for the mobility of clusters on surfaces.

The Co nanoparticles were generated by DC magnetron sputtering of a cobalt target (99.95 % purity) in 1.0 Torr of ultraclean argon ($<$ 1 ppb) and a baked ultra high vacuum (UHV) chamber (base pressure in the high 10^{-10} Torr range). This sputter chamber is attached to a UHV compatible transmission electron microscope (TEM) (modified JEOL 200CX [11], base pressure in the low 10^{-9} Torr range) via a connecting tube. After sputtering for 30 s in the static argon atmosphere, the argon gas was pumped out through the microscope and the particles were deposited on the substrate. The temperature of the substrate could be regulated with an accuracy of 20 K. Details of the instrument have been described elsewhere [12]. The Cu and Ag substrates were produced as single crystalline films, 50 - 100 nm thick, by e-beam evaporation on (100) rocksalt in a UHV system. Subsequently they were mounted on Si support rings and transferred into the microscope. Any possible oxide on the films was reduced in-situ: by heating in vacuum to 800 K in the case of Ag, and by heating in methanol vapor at 600 K in the case of Cu [13,14].

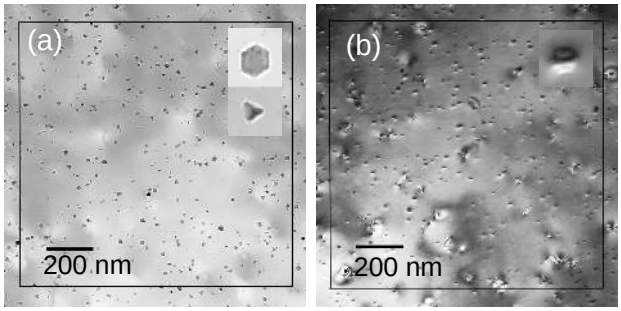

FIG. 1. In-situ TEM bright field images of Co nanoparticles on Cu(100) at 300 K (a) and at 600 K (b). The images show representative areas of the samples used for the AFM scans in Fig. 2. The particle coverage is identical within 5%. The inserts show enlargements of typical clusters.

Co clusters were first deposited at room temperature on a clean Cu(100) surface in the UHV TEM. The films could be imaged within about one minute of deposition. The particles were randomly distributed, and their size distribution was log-normal with a mean particle diameter of 13 nm and a variance of 4 nm. Bright field images shown in Fig. 1(a) together with dark field images and selected area diffraction patterns (not shown) indicated that the particles were randomly oriented with respect to the substrate. In the diffraction pattern the first four fcc rings were visible. The (220) ring was much stronger than the (200) ring, which indicates a $\langle 111 \rangle$ texture of the particles. This agrees with their highly faceted shape seen in bright field (Fig. 1(a)), assuming that they are faceted along $\langle 111 \rangle$.

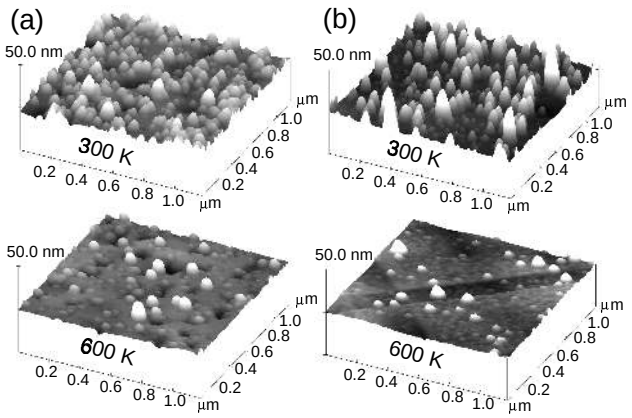

FIG. 2. Tapping mode AFM scans for Co nanoparticles deposited on Cu(100) (a) and Ag(100) (b) at 300 and 600 K. At room temperature all particles are sitting on the surface, whereas the majority of them burrowed into the substrate at 600 K.

Particles were then deposited with equal coverage on a substrate held at 600 K, which are shown in bright field in Fig. 1(b). Note that the particle size distribution remained unchanged. The vast majority of the Co particles became epitaxial with the Cu(100) film, assuming the substrate orientation. The particles were dislocation free, and since the lattice constant of Co is 1.9 % smaller than Cu, they strained the Cu matrix. Formation of coherent, dislocation free Co islands on Cu, up to 37.5 nm in radius, were also reported for the vapor deposition of Co onto Cu (100) at 620 K [15]. Notably the image contrast observed in Fig. 1(b) resembles the image contrast of coherent Co precipitates embedded in a Cu matrix calculated by Ashby and Brown [16], providing initial evidence that the nanoparticles were below the top surface of the film.

Ex-situ atomic force microscopy (AFM) scans on the non electron transparent part of the TEM specimens, performed in tapping mode, revealed a pronounced difference in the surface topographies for the 300 and 600 K depositions, as seen in Fig. 2(a). Whereas all particles reside on the surface after deposition at room temperature, the majority of them has sunk into the substrate after deposition at 600 K. Energy dispersive X-ray analysis (EDX) and electron energy loss spectrometry (EELS) measurements confirm that the topography change was due to the Co particles sinking rather than spreading over the surface. Fig. 2 also shows that a small fraction of the particles deposited at 600 K did not sink. We attribute this observation to residual contamination on the film. The height to height correlation functions of the two samples shown in Fig. 3(a), $H(|\vec{r}|) = \langle [z(\vec{r}_0) - z(\vec{r}_0 + \vec{r})]^2 \rangle$ (the brackets denote an average over all possible $\vec{r}_0$ and a spherical average over $\vec{r}$), have almost identical shapes, but with the RMS roughness being reduced by a factor of 2 for deposition at 600 K. There are no correlations in interparticle distances, again showing that they are randomly located on the surface. It should also be noted that the characteristic length scale derived from these graphs does not correspond to the actual particle size but to the size of the AFM tip. Coverage in the AFM images appears much higher than in the TEM micrographs for this reason.

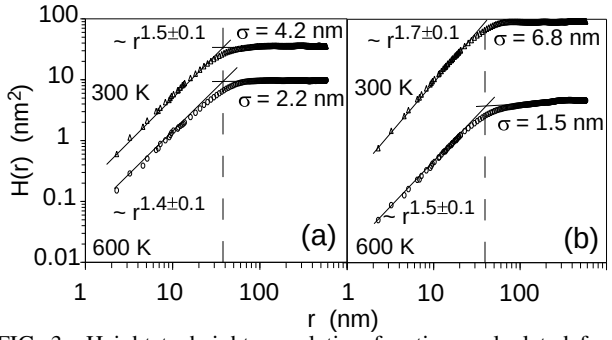

FIG. 3. Height to height correlation functions calculated from AFM images of Co on Cu (a) and Ag (b). The characteristic length scale in both images is around 40 nm and determined by the AFM tip. Beyond that there is no sign of any correlation between particles. All curves rise roughly with the $r^{1.6}$ dependence expected for a spherical AFM tip. The values of the RMS roughness σ are directly comparable within (a) and (b) since the 300 K and 600 K samples of each substrate material had an identical coverage ($\pm$ 5 %).

Despite the lattice mismatch of 13 % between Co and Ag, this system behaved very much like Co-Cu. The particles were randomly oriented on the Ag(100) film after deposition at room temperature, while after deposition at 600 K they again assumed the (100) orientation of the substrate. Also, the ex-situ AFM measurements on the two samples in Fig. 2(b) show that the majority of the Co cluster sank after deposition at 600 K, but not after deposition at 300 K. The height to height correlation functions (Fig. 3(b)) also show a reduced roughness at 600 K, and no correlation between particles. To further confirm these results, a Ag film with Co clusters deposited at 600 K was prepared in a cross-sectional geometry and analyzed by EDX. Care had been taken to align the surface of the Ag film parallel to the electron beam. The map of the Co EDX signal, illustrated in the top right corner of Fig. 4, shows 5 Co clusters in the field of view. Linescans of the Co and Ag signal through the particles along the film normal, included at the bottom of Fig. 4, show more clearly that the

particles are located just below the top surface of the film, not merely capped by substrate atoms.

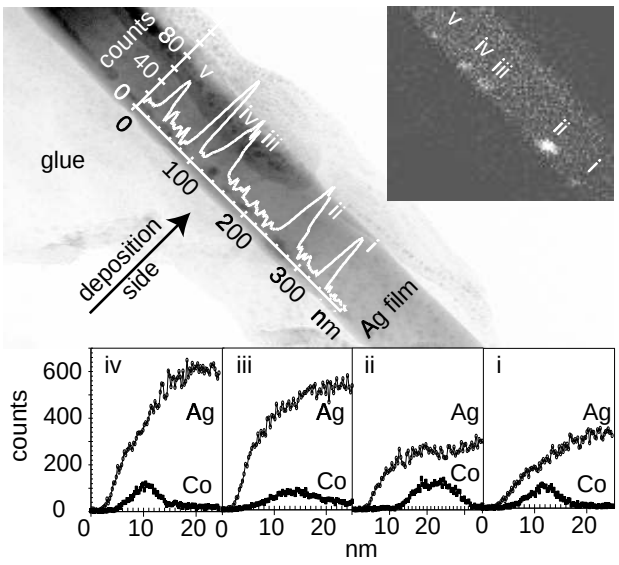

FIG. 4. Cross-sectional TEM micrograph of Co on Ag(100) at 600 K combined with EDX data. The insert in the top right corner shows the spatial distribution of the Co EDX signal across the film. Also shown are a line profile of the Co intensity parallel to the surface (overlayed the TEM image) and of the Ag and Co intensities through particles i – iv along the film normal. They confirm that the particles are located just below the surface; scan ii is slightly off center, which explains the apparent greater depth of particle ii.

The basic driving force for this sinking process is, of course, the reduction in total free energy by exchanging the Co-vacuum interface above the surface with a Co-substrate interface below the surface without increasing the substrate surface area. This process is likely to occur in two steps; first by the coating of the particle with substrate material, as suggested by Ref. [1–10], followed by burrowing. We illustrate the savings in free energy by these two processes for the case of Co particles on Ag. By coating the Co particle with Ag, the reduction in energy per unit area, $\Delta\gamma$, is:

$$\Delta\gamma = \gamma_{Co} - (\gamma_{Ag} + \gamma_{Ag-Co} + \gamma_{chem}) \qquad (1)$$

The surface energy γ_{Ag} of Ag(100) is 1.2 $\mathrm{J/m^2}$ [17] while for Co we choose the lowest energy surface (0001) for which γ_{Co} is 2.8 $\mathrm{J/m^2}$ [17]. The energy associated with the semi-coherent Co-Ag interface is approximated by the average of the high-angle grain boundary energies of Co and Ag, γ_{Ag-Co}, 0.6 $\mathrm{J/m^2}$ [18], plus an additional term accounting for the immiscibility at the interface. We estimate this term, γ_{chem}, using the zero-layer model due to Becker [19], such that $\gamma_{chem} = 2g\Omega N_S$, where g is a geometric factor ($\approx 1/3$), Ω is the heat of mixing parameter, 0.2 $\mathrm{eV/atom}$ [20], and N_S is the area density of atoms on the interface, 1×10^{19} $\mathrm{m^{-2}}$. With this set of values, $\Delta\gamma$ equates to 0.8 $\mathrm{J/m^2}$.

By particle burrowing an additional amount γ_{Ag} (rather than merely $\Delta\gamma$) is gained in free energy per unit area. For particles with nanodimensions, the capillary forces associated with this reduction in surface area are on the order of the theoretical strength of the material [21]. We have estimated the rate at which nanoparticles enter into the substrate by assuming that Ag atoms diffuse from under the Co cluster to the surface along the Ag / Co interface of width δ. With the reasonable assumption that the Co cluster remains nearly spherical, it is straightforward to show using the procedure of Chu et al. [22] for the sintering of two spheres that the time t required for the cluster to burrow to a depth equal to 99 % of its diameter is:

$$t = \alpha \frac{kT}{V_m \gamma_{Ag} \delta D} r^4 \qquad (2)$$

α is a geometric factor, which has a value of 0.8 in this case. V_m is the volume of one substrate atom and D the diffusion coefficient along the Ag / Co interface. T is the substrate temperature and k the Boltzmann constant. The same dependencies on r, D, and γ_{Ag} in Eq. (2) are typical for processes that are dominated by surface or interface diffusion but with different boundary conditions having different numerical factors α. The time for two spheres of radius r to sinter and form one sphere by surface diffusion is given by Eq. (2) but with $\alpha = 0.6$ [23], while Coble creep [24] is described by Eq. (2) with $\alpha = 0.2$ [25].

With the approximation that the diffusion coefficient D in Eq. (2) along the cluster substrate interface is equal to the geometric average of grain boundary self-diffusion at 600 K in polycrystalline Ag, $\delta D = 2.9 \times 10^{-22}$ $\mathrm{m^3 s^{-1}}$ [26], and Co, $\delta D = 7.6 \times 10^{-25}$ $\mathrm{m^3 s^{-1}}$ [27], Eq. (2) yields a time of less than 0.1 s for a cluster of 13 nm to sink into the substrate. At room temperature, on the other hand, the time required is of the order of months. These rates fit nicely with our observations that no burrowing is observed at room temperature even after 10^4 s, while it occurs in less than 100 s at 600 K. The r^4-dependence in Eq. (2) explains, moreover, why this phenomenon has not been observed for larger particles. Note that increasing the particle size from 10 nm to 1 μm slows the sinking time by a factor of 10^8, whereas increasing the temperature from 600 K to even the melting point only gains a factor of 10^4.

The situation is somewhat more complicated for Co clusters on Cu(100) since the particle becomes coherent with the substrate. The strain energy, however, is not significant for these small particle sizes. The strain energy of a spherical Co cluster embedded coherently in a Cu matrix is only 5×10^{-4} $\mathrm{eV/\AA^{-3}}$ times the cluster volume [28]. For a cluster close to the surface we confirmed by computer simulations that the strain energy is, in good approximation, proportional to the cluster volume already embedded in the film. Thus the strain energy only becomes significant for particles much larger than those in these experiments. The surface energies involved ($\gamma_{Cu(100)}$ = 2.2 $\mathrm{J/m^2}$ [17] , $\gamma_{Cu-Co(coherent)}$ = 0.02 $\mathrm{J/m^2}$ [18], γ_{chem} = 0.1 $\mathrm{J/m^2}$ [20]) again predict that the Co cluster will acquire an initial Cu coating. The burrowing time according to Eq. (2) and δD approximated by the geometric average of Co and Cu

grain boundary diffusivity (δD(Cu) = 2.8×10^{-24} $\mathrm{m}^3\mathrm{s}^{-1}$ at 600 K [27]), is less than 1 s. Since the Co particle reorients to become coherent with the Cu matrix, however, the diffusion along the Cu / Co interface may in fact be slower. The reorientation process itself was also rapid and was completed already by the time the particles could be imaged.

Finally we argue against an alternative pathway that could lead to buried clusters. The clusters in principle can become buried on a local scale by surface diffusion of substrate atoms onto the side of the clusters. This surface structure would have thickness variations of the order of the average particle size unless they were further smoothened by the process suggested in Ref. [10], where atoms from the bottom part of the film diffuse through holes in the film to fill the space between particles. In analogy to Eq. (2) we estimate that this process would be a factor of 10^5 to 10^7 times slower than the burrowing on the basis of the lengthscales involved, which would be the interparticle distance for the driving force and the hole distance for the amount of material that has to be supplied. This slower rate is not offset by the faster surface diffusion. This mechanism, moreover, has other difficulties to explain our specific results: (i) particles still remaining on the surface as seen in Fig. (2) could not be explained and (ii) Ref. [6,10] do not observe diffusion through pinholes at temperatures as low as 600 K. Therefore we exclude this process here.

In conclusion, we have presented experimental evidence that Co nanoparticles in the 10 nm size regime sink below the surface when deposited on Ag(100) and Cu(100) surfaces at 600 K, and that this process is likely due to burrowing. Burrowing is driven by the extremely large capillary forces on the particles. This work suggests that burrowing should occur in all systems where the nanoparticles have a significantly higher surface energy than the substrate. If the particle had a smaller surface energy, it would simply wet the substrate. Immiscibility is not an essential feature.

We are grateful to N. Finnigan, T. Banks, S. Mayr and R. Twesten for their help in characterizing our samples. The research was supported by the Department of Energy under grant DEFG-96ER45439. Extensive use was made of the DOE supported Center for Microanalysis of Materials at UIUC. A grant of computer time from the National Center for Supercomputing Applications (NCSA) at UIUC is also acknowledged.

[1] A. Rolland and B. Aufray, Surf. Sci. **162**, 530 (1985).
[2] B. Aufray *et al.*, Surf. Sci. **307 - 309**, 531 (1994).
[3] J. M. Roussel *et al.*, Surf. Sci. **352 - 354**, 562 (1996).
[4] G. Tréglia and B. Legrand, Phys. Rev. B **35**, 4338 (1987).
[5] J. M. Roussel *et al.*, Phys. Rev. B **55**, 10931 (1997).
[6] H .Li and B. P. Tonner, Surf. Sci. **237**, 141 (1990).
[7] A. K. Schmid *et al.*, Phys. Rev. B **48**, 4338 (1993).
[8] J. de la Figuera *et al.*, Surf. Sci. **307 - 309**, 538 (1994).
[9] M. Ø. Pedersen *et al.*, Surf. Sci. **387**, 86 (1997).
[10] G. L. Zhou, M. H. Yang and C. P. Flynn, Phys. Rev. Lett. **77**, 4580 (1996).
[11] M. L. McDonald, J. M. Gibson and F. C. Unterwald, Rev. Sci. Instrum. **60**, 700 (1989).
[12] D. L. Olynick, J. M. Gibson and R. S. Averback, Mater. Sci. Eng. A **204**, 54 (1995).
[13] S. M. Francis *et al.*, Surf. Sci. **315**, 284 (1994).
[14] J. C. Yang *et al.*, Appl. Phys. Lett. **70**, 3522 (1997).
[15] W. J. Jesser and J. W. Matthews, Phil. Mag. **17**, 461 (1968).
[16] M. F. Ashby and L. M. Brown, Phil. Mag. **8**, 1083 (1963).
[17] L. Vitos *et al.*, Surf. Sci. **411**, 186 (1998).
[18] L. E. Murr, *Interfacial Phenomena in Metals and Alloys*, (Addison-Wesley, Reading, Massachusetts, 1975).
[19] R. Becker, Ann. Phys. **32**, 128 (1938).
[20] A. K. Niessen *et al.*, CALPHAD **7**, 51 (1983).
[21] Z. Huilong, R. S. Averback, Phil. Mag. Lett. **73**, 27 (1996); Our MD simulations predict a pressure of 5 GPa at the bottom interface of a 5nm Co cluster in Cu.
[22] M. Y. Chu *et al.*, J. Am. Ceram. Soc. **74**,1217 (1991).
[23] J. R. Blachere, A. Sedehi and Z. H. Meiksin, J. Mater. Sci. **19**, 1202 (1984).
[24] R. L. Coble, J. Appl. Phys. **34**, 1679 (1963).
[25] The local stress normal to the boundary is assumed to be $2\gamma/r$.
[26] P. Gas and J. Bernardini, Surf. Sci. **72**, 365 (1978).
[27] I. Kaur, W. Gust and L. Kozma, *Handbook of Grain and Interface Boundary Diffusion Data*, (Ziegler, Stuttgart, 1989).
[28] J. D. Eshelby, in *Solid State Physics*, edited by F. Seitz and D. Turnbull (Academic Press, New York, 1956), Vol. 3, p. 79.